Journal of Marine Science and Technology

Volume 21 | Issue 3 Article 2

SHAPE OPTIMIZATION OF MULTI-CHAMBER SIDE INLET/OUTLET MUFFLERS HYBRIDIZED WITH MULTIPLE PERFORATED INTRUDING TUBES USING A GENETIC ALGORITHM

Min-Chie Chiu
Department of Mechanical and Automation Engineering, Chun Chiu University of Science and Technology, Changhua County, Taiwan, R.O.C, minchie.chiu@msa.hinet.net

Ying-Chun Chang
Department of Mechanical Engineering, Tatung University, Taipei, Taiwan, R.O.C

SHAPE OPTIMIZATION OF MULTI-CHAMBER SIDE INLET/OUTLET MUFFLERS HYBRIDIZED WITH MULTIPLE PERFORATED INTRUDING TUBES USING A GENETIC ALGORITHM

Acknowledgements

The authors acknowledge the financial support of the National Science Council (NSC97-2221-E-235-001, Taiwan, ROC)

Journal of Marine Science and Technology, Vol. 21, No. 3, pp. 238-249 (2013)
DOI: 10.6119/JMST-012-0314-1

SHAPE OPTIMIZATION OF MULTI-CHAMBER SIDE INLET/OUTLET MUFFLERS HYBRIDIZED WITH MULTIPLE PERFORATED INTRUDING TUBES USING A GENETIC ALGORITHM

Min-Chie Chiu[1] and Ying-Chun Chang[2]

Key words: perforated intruding tube, decoupled numerical method, space constraints, genetic algorithm.

ABSTRACT

The use of perforated-tube side mufflers for depressing venting noise within a constrained space has been prevalent in modern industries. Also, research on mufflers equipped with side inlets/outlets has been thoroughly documented. However, research on shape optimization of side inlet/outlet mufflers hybridized with multiple open-ended perforated intruding tubes which may enhance acoustic performance has gone unnoticed. Therefore, we wish to not only analyze the sound transmission loss (STL) of side inlet/outlet mufflers but also to optimize their best design shape within a limited space.

In this paper, the generalized decoupling technique and the plane wave theory used in solving the coupled acoustical problem are employed. Also, a four-pole system matrix for evaluating acoustic performance is deduced in conjunction with a genetic algorithm (GA). We have also introduced a numerical study that deals with broadband noise within a constrained blower room using three kinds of mufflers. Additionally, before muffler shape optimization is performed, an accuracy check on the mathematical models has been performed. Moreover, to verify the reliability of the GA optimization, optimal noise abatements for various pure tones on various mufflers have been examined. Results reveal that mufflers equipped with perforated intruding tubes are superior to those equipped with non-perforated intruding tubes. Also, mufflers with multi-perforated tubes will increase the acoustic performance. Consequently, the approach used in seeking the optimal design of the STL proposed in this study is quite effective.

I. INTRODUCTION

Research on mufflers was started by Davis *et al.* in 1954 [5]. A side inlet/outlet muffler is customarily used [9] when dealing with horizontal industrial noise emitted from a perpendicular vertical system in the low frequency range. Because the constrained problem is mostly concerned with the necessity of operation and maintenance in practical engineering work, there is a growing need to optimize acoustical performance within a limited space. In previous work, the shape optimization of mufflers equipped with an internal non-perforated tube has been discussed [1, 3, 11, 22]. However, the acoustical performance is still insufficient.

Based on the coupled equations, an assessment of a new acoustical element (internal perforated tube) which will improve the acoustical performance for mufflers was discussed by Sullivan and Crocker in 1978 [18]. A series of theory and numerical techniques in decoupling the acoustical problems have been proposed [14-17, 19]. In 1981, Jayaraman and Yam [7] developed a method for finding an analytical solution; however, a presumption of the velocity equality within the inner and outer duct, which is not reasonable in the real world, is required. To overcome this drawback, Munjal *et al*. [12] provided a generalized de-coupling method. Regarding the flowing effect, Peat [13] publicized the numerical decoupling method by finding the eigen value in transfer matrices. In order to maintain a steady volume-flow-rate in a venting system, a muffler's back pressure within an allowable range is compulsory. Therefore, Wang [20] developed an open-ended perforated intruding-tube muffler, a low back-pressure muffler with non-plug tubes inside the cavity, using the *BEM* (Boundary Element Method). However, the need to investigate the optimal muffler design under space constraints was neglected.

To increase acoustical performance, three kinds of five-chamber side inlet mufflers (a muffler hybridized with four

Paper submitted 11/06/10; revised 11/04/11; accepted 03/14/12. Author for correspondence: Min-Chie Chiu (e-mail: minchie.chiu@msa.hinet.net).
[1]Department of Mechanical and Automation Engineering, Chun Chiu University of Science and Technology, Changhua County, Taiwan, R.O.C.
[2]Department of Mechanical Engineering, Tatung University, Taipei, Taiwan, R.O.C.

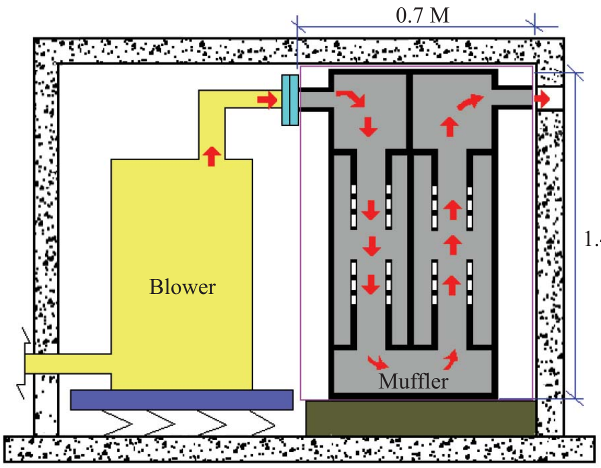

Fig. 1. A blower within a constrained machine room.

perforated intruding tubes, a muffler hybridized with two perforated tubes and two non-perforated tubes, and a muffler hybridized with four non-perforated tubes) with lower back pressure are adopted. A shape optimization of five-chamber side inlet mufflers that deal with broadband noise within a constrained blower room has been investigated by using a four-pole system matrix in conjunction with a decoupled numerical method. Moreover, a genetic algorithm (*GA*), a robust scheme used to search for the global optimum by imitating a genetic evolutionary process, has been used during the optimization process. Before the shape optimization of the mufflers, a reliability check of the *GA* optimization for various pure tones (300 Hz, 600 Hz, and 900 Hz) on various mufflers is performed.

II. THEORETICAL BACKGROUND

In this paper, three kinds of five-chamber side inlet/outlet mufflers (hybridized with four perforated intruding tubes, two perforated + two non-perforated tubes, and four non-perforated intruding tubes) were adopted for noise abatement on the constrained blower room shown in Fig. 1. The outlines of these mufflers as noise-reduction devices are shown in Figs. 2(a), 2(b), and 2(c). The acoustical fields with respect to various mufflers are shown in Figs. 3(a), 3(b) and 3(c).

As indicated in Figs. 2(a) and 3(a), the five-chamber side inlet/outlet muffler equipped with four perforated intruding tubes, which is composed of twenty-one acoustical elements, has seven categories of components — eleven straight ducts (I), two side-inlet tubes (II), two side-outlet tubes (III), one simple contracted element (IV), one simple expanded element (V), one expanded perforated intruding tube (VI), and one contracted perforated intruding tube (VII). As indicated in Figs. 2(b) and 3(b), the five-chamber side inlet/outlet muffler equipped with two perforated intruding tubes and two non-perforated intruding tubes has nine categories of components — eleven straight ducts (I), two side-inlet tubes (II) , two side-outlet tubes (III), one simple contracted element (IV), one simple expanded element (V), one expanded perforated intruding tube (VI), one contracted perforated intruding tube (VII), one contracted non-perforated intruding tube (VIII), and one expanded non-perforated intruding tube (IX). Moreover, for a muffler equipped with four non-perforated intruding tubes, there are nine categories of components — eleven

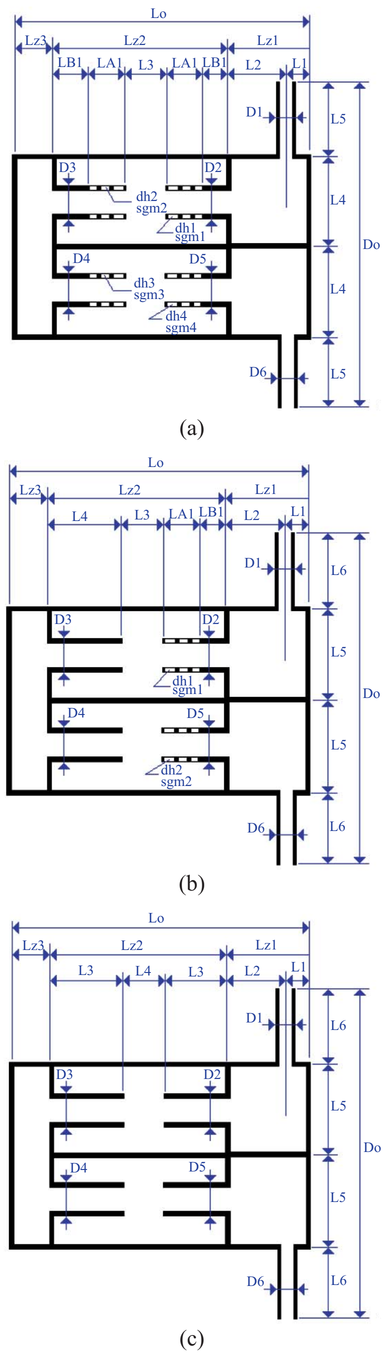

Fig. 2. The outline of a five-chamber side inlet/outlet muffler hybridized with perforated/non-perforated intruding tubes: (a) four perforated intruding tubes; (b) two perforated and two non-perforated intruding tubes; (c) four non-perforated intruding tubes.

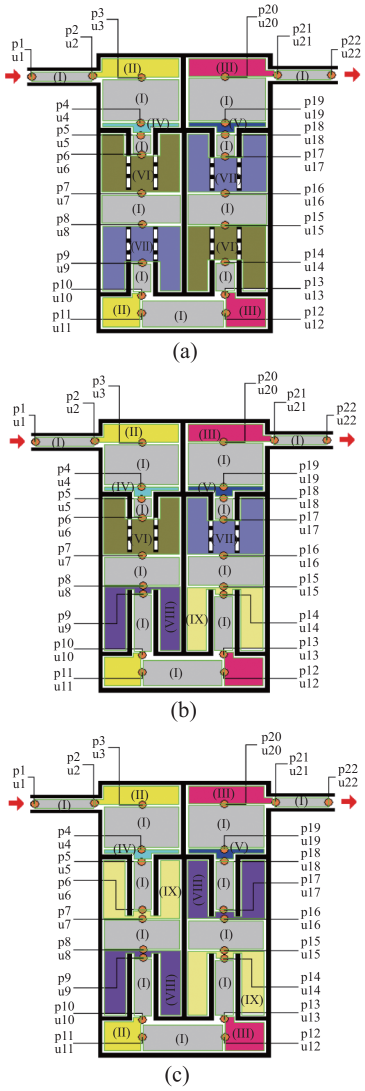

Fig. 3. Acoustical elements and nodes represented in the acoustical field for a five-chamber side inlet/outlet muffler hybridized with perforated/non-perforated intruding tubes: (a) four perforated intruding tubes; (b) two perforated and two non-perforated intruding tubes; (c) four non-perforated intruding tubes.

straight ducts, two side-inlet tubes, two side-outlet tubes, one simple contracted element, one simple expanded element, one expanded perforated intruding tube, one contracted perforated intruding tube, one contracted non-perforated intruding tube, and one expanded non-perforated intruding tube — which are shown in Figs. 2(c) and 3(c).

The related acoustic pressure p and acoustic particle velocity u within the mufflers are also represented by twenty-two nodes. The detailed mathematical derivation of various muffler systems is presented below.

1. A Side Inlet/Outlet Muffler Hybridized with Four Perforated Intruding Tubes

As derived in previous work [1, 3, 10-13, 18, 22], individual transfer matrixes with respect to straight ducts, side inlet/outlet tubes, simple expansion/contracted tubes, and perforated expanded/contracted intruding tubes are described as follows:

$$\begin{pmatrix} p_i \\ \rho_o c_o u_i \end{pmatrix} = \begin{bmatrix} T_{(i)xx} & T_{(i)xy} \\ T_{(i)yx} & T_{(i)yy} \end{bmatrix} \begin{pmatrix} p_{i+1} \\ \rho_o c_o u_{i+1} \end{pmatrix} \tag{1a}$$

where

$$i\text{: odd number at } 1, 3, 5, \ldots, 21 \tag{1b}$$

$$\begin{pmatrix} p_j \\ \rho_o c_o u_j \end{pmatrix} = \begin{bmatrix} T_{(j)xx} & T_{(j)xy} \\ T_{(j)yx} & T_{(j)yy} \end{bmatrix} \begin{pmatrix} p_{j+1} \\ \rho_o c_o u_{j+1} \end{pmatrix} \tag{2a}$$

where

$$j\text{: even number at } 2, 4, 6, \ldots, 20 \tag{2b}$$

The total transfer matrix assembled by multiplication is simplified as

$$\begin{Bmatrix} p_1 \\ \rho_o c_o u_1 \end{Bmatrix} = \prod_m \left[T_m(f) \right] \begin{Bmatrix} p_{22} \\ \rho_o c_o u_{22} \end{Bmatrix} \tag{3}$$

The sound transmission loss (STL) of a muffler is defined as [10]

$$STL_1(Q, f, Af_1, Af_2, Af_3, Af_4, Af_5, Af_6, Af_7, Af_8, Af_9, Af_{10}, Af_{11}, Af_{12}, Af_{13}, Af_{14}, Af_{15}, Af_{16}, Af_{17}, Af_{18})$$

$$= 20\log\left(\frac{\left| T_{11}^* + T_{12}^* + T_{21}^* + T_{22}^* \right|}{2} \right) + 10\log\left(\frac{S_1}{S_{21}} \right) \tag{4a}$$

where

$$Lz_2 = Af_1;\ Lz_3 = Af_2;\ L_1 = Af_3;\ L_3 = Af_4{*}Lz_2;\ L_{A1} = Af_5{*}(Lz_3\text{-}L_3)/2;$$
$$L_4 = Af_6;\ dh_1 = Af_7;\ sgm_1 = Af_8;\ dh_2 = Af_9;\ sgm_2 = Af_{10};\ dh_3 = Af_{11};$$
$$sgm_3 = Af_{12};\ dh_4 = Af_{13};\ sgm_4 = Af_{14};\ D_2 = Af_{15}{*}L_6;\ D_3 = Af_{16}{*}L_6;$$
$$D_4 = D_3;\ D_5 = Af_{17}{*}L_6;\ D_6 = Af_{18} \tag{4b}$$

2. A Side Inlet/Outlet Muffler Hybridized with Two Perforated Intruding Tubes and Two Non-Perforated Intruding Tubes

Similarly, as indicated in section II.1, the total transfer matrix assembled by multiplication is

$$\begin{pmatrix} p_1 \\ \rho_o c_o u_1 \end{pmatrix} = \prod_m \left[T_m(f) \right] \begin{Bmatrix} p_{22} \\ \rho_o c_o u_{22} \end{Bmatrix} \tag{5}$$

The sound transmission loss (*STL*) of a muffler is defined as [10]

$$STL_2(Q,\ f,\ Af_1,\ Af_2,\ Af_3,\ Af_4,\ Af_5,\ Af_6,\ Af_7,\ Af_8,\ Af_9, Af_{10},$$
$$Af_{11},\ Af_{12},\ Af_{13},\ Af_{14},\ Af_{15})$$
$$= 20\log\left(\frac{\left|T_{11}^{**}+T_{12}^{**}+T_{21}^{**}+T_{22}^{**}\right|}{2}\right)+10\log\left(\frac{S_1}{S_{21}}\right) \quad (6a)$$

where

$Lz_2 = Af_1$; $Lz_3 = Af_2$; $L_1 = Af_3$; $L_3 = Af_4{*}Lz_2$; $L_{A1} = Af_5{*}L_4$;
$L_5 = Af_6$; $dh_1 = Af_7$; $sgm_1 = Af_8$; $dh_2 = Af_9$; $sgm_2 = Af_{10}$;
$D_2 = Af_{11}{*}L_5$; $D_3 = Af_{12}{*}L_5$; $D_4 = Af_{13}{*}L_5$; $D_5 = Af_{14}{*}L_5$;
$D_6 = Af_{15}$ (6b)

3. A Side Inlet/Outlet Muffler Hybridized with Four Non-Perforated Intruding Tubes

Likewise, as indicated in section 2.1, the total transfer matrix assembled by multiplication is

$$\begin{pmatrix} p_1 \\ \rho_o c_o u_1 \end{pmatrix} = \prod_m \left[T_m(f)\right] \begin{Bmatrix} p_{22} \\ \rho_o c_o u_{22} \end{Bmatrix} \quad (7)$$

The sound transmission loss (*STL*) of a muffler is defined as [10]

$$STL_3(Q,\ f,\ Af_1,\ Af_2,\ Af_3,\ Af_4,\ Af_5,\ Af_6,\ Af_7,\ Af_8,\ Af_9,\ Af_{10})$$
$$= 20\log\left(\frac{\left|T_{11}^{***}+T_{12}^{***}+T_{21}^{***}+T_{22}^{***}\right|}{2}\right)+10\log\left(\frac{S_1}{S_{21}}\right) \quad (8a)$$

where

$Lz_2 = Af_1$; $Lz_3 = Af_2$; $L_1 = Af_3$; $L_4 = Af_4{*}Lz_2$; $L_5 = Af_5$;
$D_2 = Af_6{*}L_6$; $D_3 = Af_7{*}L_6$; $D_4 = Af_8{*}L_6$; $D_5 = Af_9{*}L_6$; $D_6 = Af_{10}$ (8b)

4. Objective Function

By using the formulas of Eqs. (4) (6) (8), the objective function used in the *GA* optimization with respect to each type of muffler was established. For a five-chamber side inlet/outlet muffler hybridized with four perforated intruding tubes, the objective function in maximizing the *STL* at a pure tone (f) is

$$OBJ_{11} = STL_1(Q,\ f,\ Af_1,\ Af_2,\ Af_3,\ Af_4,\ Af_5,\ Af_6,\ Af_7,\ Af_8,$$
$$Af_9,\ Af_{10},\ Af_{11},\ Af_{12},\ Af_{13},\ Af_{14},\ Af_{15},\ Af_{16},\ Af_{17},\ Af_{18}) \quad (9)$$

The objective function in minimizing the broadband *SWL* is

$$OBJ_{12} = SWL_T(Q,\ Af_1,\ Af_2,\ Af_3,\ Af_4,\ Af_5,\ Af_6,\ Af_7,\ Af_8,\ Af_9,$$
$$Af_{10},\ Af_{11},\ Af_{12},\ Af_{13},\ Af_{14},\ Af_{15},\ Af_{16},\ Af_{17},\ Af_{18}) \quad (10a)$$

where

$$SWL_T = 10*\log_{10}\left\{\begin{matrix} 10^{[SWLO(f=125)-STL_1(f=125)]/10} + 10^{[SWLO(f=250)-STL_1(f=250)]/10} \\ +10^{[SWLO(f=500)-STL_1(f=500)]/10} + 10^{[SWLO(f=1000)-STL_1(f=1000)]/10} \end{matrix}\right\} \quad (10b)$$

Here, frequencies of 125 Hz, 250 Hz, 500 Hz, and 1000 Hz are the central frequencies for the corresponding bands.

For a five-chamber side inlet/outlet muffler hybridized with two perforated intruding tubes and two non-perforated intruding tubes, the objective function in maximizing the *STL* at a pure tone (f) is

$$OBJ_{21} = STL_2(Q,\ f,\ Af_1,\ Af_2,\ Af_3,\ Af_4,\ Af_5,\ Af_6,\ Af_7,\ Af_8,$$
$$Af_9,\ Af_{10},\ Af_{11},\ Af_{12},\ Af_{13},\ Af_{14},\ Af_{15}) \quad (11)$$

Similarly, the objective function in minimizing the broadband *SWL* is

$$OBJ_{22} = SWL_T(Q,\ Af_1,\ Af_2,\ Af_3,\ Af_4,\ Af_5,\ Af_6,\ Af_7,\ Af_8,\ Af_9,$$
$$Af_{10},\ Af_{11},\ Af_{12},\ Af_{13},\ Af_{14},\ Af_{15}) \quad (12)$$

For a five-chamber side inlet/outlet muffler hybridized with four non-perforated intruding tubes, the objective function in maximizing the *STL* at a pure tone (f) is

$$OBJ_{31} = STL_3(Q,\ f,\ Af_1,\ Af_2,\ Af_3,\ Af_4,\ Af_5,\ Af_6,\ Af_7,$$
$$Af_8,\ Af_9,\ Af_{10}) \quad (13)$$

Likewise, the objective function in minimizing the broadband *SWL* is

$$OBJ_{32} = SWL_T(Q,\ f,\ Af_1,\ Af_2,\ Af_3,\ Af_4,\ Af_5,\ Af_6,\ Af_7,$$
$$Af_8,\ Af_9,\ Af_{10}) \quad (14)$$

The related ranges of parameters with respect to three kinds of mufflers are shown in Table 1.

III. MODEL CHECK

Before performing the *GA* optimal simulation on mufflers, an accuracy check of the mathematical models on three kinds of fundamental acoustical elements that include (1) a

Table 1. Range of design parameters for three kinds of side inlet/outlet mufflers hybridized with perforated/non-perforated intruding tubes.

Muffler type	Range of design parameters
muffler (A)	*Lo* = 1.4(m); *Do* = 0.7(m); *Q* = 0.02 (m^3/s); D_1 = 0.0508 (m); Af_1: [0.5, 0.8], Af_2 = [0.1, 0.2], Af_3 = [0.08, 0.2]; Af_4 = [0.1, 0.9]; Af_5 = [0.1, 0.9]; Af_6 = [0.2, 0.3]; Af_7 = [0.00175, 0.007]; Af_8 = [0.03, 0.1]; Af_9 = [0.00175, 0.007]; Af_{10} = [0.03, 0.1]; Af_{11} = [0.00175, 0.007]; Af_{12} = [0.03, 0.1]; Af_{13} = [0.00175, 0.007]; Af_{14} = [0.03, 0.1]; Af_{15} = [0.2, 0.9]; Af_{16} = [0.03, 0.1]; Af_{17} = [0.2, 0.9]; Af_{18} = [0.0508, 0.1]
muffler (B)	*Lo* = 1.4(m); *Do* = 0.7(m); *Q* = 0.02 (m^3/s); D_1 = 0.0508 (m); Aff_1: [0.5, 0.8], Aff_2 = [0.1, 0.2], Aff_3 = [0.08, 0.2]; Aff_4 = [0.1, 0.9]; Aff_5 = [0.2, 0.8]; Aff_6 = [0.2, 0.3]; Aff_7 = [0.00175, 0.007]; Aff_8 = [0.03, 0.1]; Aff_9 = [0.00175, 0.007]; Aff_{10} = [0.03, 0.1]; Aff_{11} = [0.2, 0.9]; Aff_{12} = [0.2, 0.9]; Aff_{13} = [0.2, 0.9]; Aff_{14} = [0.2, 0.9]; Aff_{15} = [0.0508, 0.1]
muffler (C)	*Lo* = 1.4(m); *Do* = 0.7(m); *Q* = 0.02 (m^3/s); D_1 = 0.0508 (m); $Afff_1$: [0.5, 0.8], $Afff_2$ = [0.1, 0.2], $Afff_3$ = [0.08, 0.2]; $Afff_4$ = [0.1, 0.9]; $Afff_5$ = [0.2, 0.3]; $Afff_6$ = [0.2, 0.9]; $Afff_7$ = [0.2, 0.9]; $Afff_8$ = [0.2, 0.9]; $Afff_9$ = [0.2, 0.9]; $Afff_{10}$ = [0.0508, 0.1]

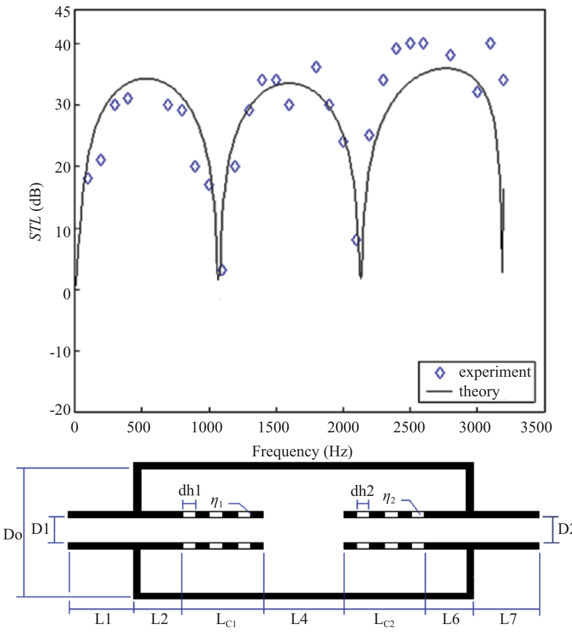

Fig. 4. Performance of a one-chamber muffler equipped with perforated intruding tubes (Experimental data is from Wang *et al.* [21]).

single-chamber muffler equipped with two perforated intruding tubes, (2) a single-chamber muffler hybridized with two non-perforated intruding tubes, and (3) a side inlet/outlet single-chamber muffler are performed using the experimental data from Wang *et al.* [21], Chang *et al.* [2], and Chiu *et al.* [4]. As depicted in Figs. 4~6, the theoretical and experimental data for the models are accurate and in agreement. Therefore, the proposed fundamental mathematical models with related acoustical components are acceptable. Consequently, the models linked with the numerical method are applied to the shape optimization of five-chamber side inlet/outlet mufflers hybridized with perforated/non-perforated intruding tubes.

IV. CASE STUDIES

The noise reduction of a space-constrained blower room is shown in Fig. 1. The sound power levels (*SWL*s) of the blower

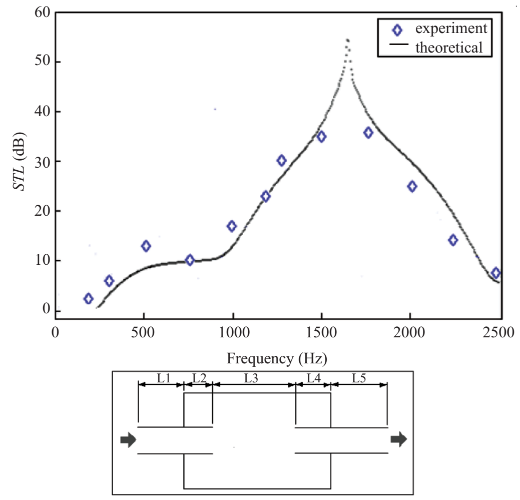

Fig. 5. Performance of a single-chamber muffler with extended tubes at the mean flow velocity of 3.4 m/sec (Experimental data is from Chang *et al.* [2]).

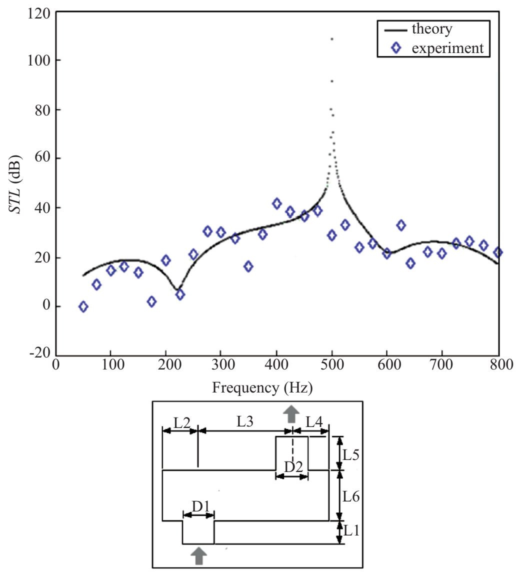

Fig. 6. Performance of single-chamber muffler with a side inlet/outlet for a stationary medium (Experiment data is from Chiu *et al.* [4]).

Table 2. Unsilenced *SWLs* of a blower inside a duct outlet.

Frequency - Hz	125	250	500	1000	overall
SWLO - dB	148	138	135	135	148.8

in lower frequencies (125 Hz, 250 Hz, 500 Hz, and 1000 Hz) at the pipe outlet of are listed in Table 2. To reduce the venting noise emitted from the blower's outlet, three kinds of low back-pressure multi-chamber mufflers — five-chamber side inlet/outlet mufflers hybridized with perforated/non-perforated intruding tubes shown in Figs. 2(a), 2(b), and 2(c) — are considered. As shown in Fig. 1, the available space for a muffler is 0.7 m in width, 0.7 m in height, and 1.4 m in length. Before the minimization of the blower's broadband noise is performed, a reliability check of the *GA* optimization for various pure tones (300 Hz, 600 Hz, and 900 Hz) on various mufflers (muffler (A), muffler (B), and muffler (C)) is made. The related flow rate (Q) and thickness of a perforated tube (t) are preset as 0.02 (m^3/s) and 0.001 (m), respectively. The corresponding *OBJ* functions, space constraints, and the ranges of design parameters are summarized in Table 1.

V. GENETIC ALGORITHMCASE STUDIES

For the optimization of the objective function (*OBJ*), the design parameters of (X_1, X_2, …, X_k) were determined [6, 8]. When the *bit* (the bit length of the chromosome) was chosen, the interval of the design parameter (X_k) with $[Lb,Ub]_k$ was then mapped to the band of the binary value. The mapping system between the variable interval of $[Lb,Ub]_k$ and the k^{th} binary chromosome of

$$[\underbrace{0\ 0\ 0\ 0\ \bullet\ \bullet\ \bullet\ 0\ 0\ 0}_{bit} \sim \underbrace{1\ 1\ 1\ 1\ \bullet\ \bullet\ \bullet\ 1\ 1\ 1}_{bit}]$$

was then built. The encoding from x to $B2D$ (binary to decimal) was performed as

$$B2D_k = \text{integer}\left\{\frac{x_k - Lb_k}{Ub_k - Lb_k}(2^{bit} - 1)\right\} \tag{15}$$

The initial population was built up by randomization. The parameter set was encoded to form a string which represented the chromosome. By evaluating the objective function (*OBJ*), the whole set of chromosomes [$B2D_1$, $B2D_2$, …., $B2D_k$] that changed from binary form to decimal form was then assigned a fitness by decoding the transformation system

$$fitness = OBJ(X_1, X_2, \ldots, X_k) \tag{16a}$$

where

$$X_k = B2D_k*(Ub_k - Lb_k)/(2^{bit}-1) + Lb_k \tag{16b}$$

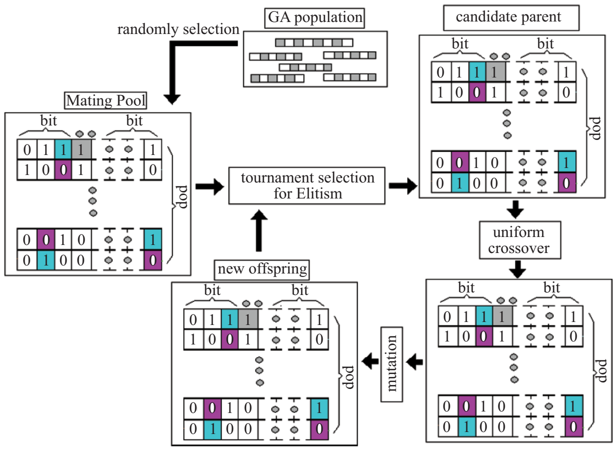

Fig. 7. Operations in the *GA* method.

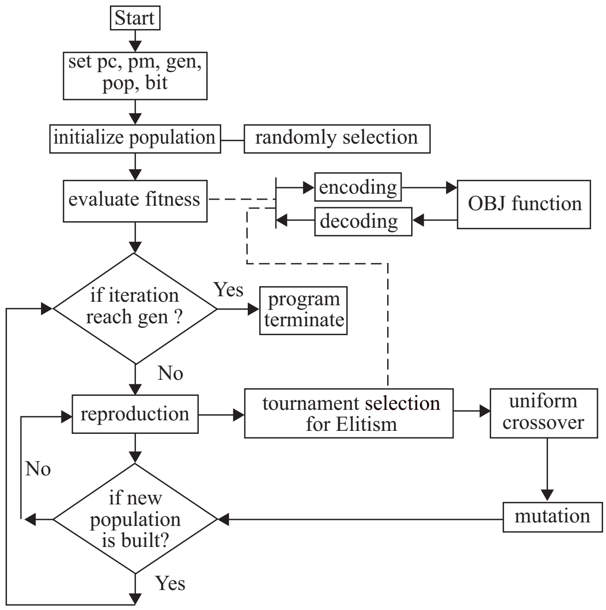

Fig. 8. The block diagram of the *GA* optimization on mufflers.

The flow diagram during a muffler's shape optimization is depicted in Fig. 7.

As indicated in Fig. 7, to process the elitism of a gene, the tournament selection, a random comparison of the relative fitness of pairs of chromosomes, was applied. During the *GA* optimization, one pair of offspring from the selected parent was generated by a uniform crossover with a probability of *pc*. Genetically, a mutation occurred with a probability of *pm* where the new and unexpected point was brought into the *GA* optimizer's search domain. To prevent the best gene from disappearing and to improve the accuracy of optimization during reproduction, an elitism scheme of keeping the best gene (one pair) in the parent generation with the tournament strategy was developed.

The process was terminated when a number of generations exceeded a pre-selected value of *gen*. The operations in the *GA* method are pictured in Fig. 8.

Table 3. Comparison of results for the variations of control parameters-*pop*, *gen*, *bit*, *pc*, *pm* in a five-chamber side inlet/outlet muffler equipped with two perforated intruding tubes and two non-perforated intruding tubes (muffler (B)) (target tone: 300 Hz).

Item	*GA* parameters						Results								
	pop	*gen*	*bit*	*pc*	*pm*	*elt*	design parameters								
1	80	25	10	0.2	0.01	1	Af_1	Af_2	Af_3	Af_4	Af_5	Af_6	Af_7	Af_8	*STL*(dB)
							0.8	0.1616	0.1731	0.1149	0.2516	0.2830	0.005573	0.0857	174.4
							Af_9	Af_{10}	Af_{11}	Af_{12}	Af_{13}	Af_{14}	Af_{15}		
							0.005137	0.03014	0.5989	0.3978	0.4634	0.2506	0.07268		
2	80	25	10	0.5	0.01	1	Af_1	Af_2	Af_3	Af_4	Af_5	Af_6	Af_7	Af_8	*STL*(dB)
							0.7534	0.1983	0.1511	0.29	0.3501	0.2699	0.003582	0.07762	199.8
							Af_9	Af_{10}	Af_{11}	Af_{12}	Af_{13}	Af_{14}	Af_{15}		
							0.003079	0.03554	0.393	0.4183	0.2801	0.627	0.0849		
3	80	25	10	0.8	0.01	1	Af_1	Af_2	Af_3	Af_4	Af_5	Af_6	Af_7	Af_8	*STL*(dB)
							0.7795	0.1858	0.1795	0.2916	0.3267	0.2082	0.00311	0.05518	216.4
							Af_9	Af_{10}	Af_{11}	Af_{12}	Af_{13}	Af_{14}	Af_{15}		
							0.006107	0.05019	0.3136	0.5839	0.3218	0.3690	0.05114		
4	80	25	10	0.9	0.01	1	Af_1	Af_2	Af_3	Af_4	Af_5	Af_6	Af_7	Af_8	*STL*(dB)
							0.7666	0.1933	0.1690	0.2415	0.6246	0.2106	0.005779	0.05121	200.8
							Af_9	Af_{10}	Af_{11}	Af_{12}	Af_{13}	Af_{14}	Af_{15}		
							0.003664	0.06065	0.3601	0.2144	0.3232	0.4114	0.06364		
5	80	25	10	0.8	0.05	1	Af_1	Af_2	Af_3	Af_4	Af_5	Af_6	Af_7	Af_8	*STL*(dB)
							0.7208	0.1475	0.1309	0.2181	0.3132	0.2022	0.002207	0.09152	219.6
							Af_9	Af_{10}	Af_{11}	Af_{12}	Af_{13}	Af_{14}	Af_{15}		
							0.006076	0.05669	0.3457	0.7611	0.4149	0.2739	0.07191		
6	80	25	10	0.8	0.09	1	Af_1	Af_2	Af_3	Af_4	Af_5	Af_6	Af_7	Af_8	*STL*(dB)
							0.7683	0.1346	0.1497	0.2681	0.2962	0.283	0.005214	0.08529	218.5
							Af_9	Af_{10}	Af_{11}	Af_{12}	Af_{13}	Af_{14}	Af_{15}		
							0.005876	0.04211	0.3163	0.6769	0.2239	0.3403	0.05479		
7	80	25	15	0.8	0.05	1	Af_1	Af_2	Af_3	Af_4	Af_5	Af_6	Af_7	Af_8	*STL*(dB)
							0.7264	0.1848	0.1947	0.2071	0.329	0.2247	0.002576	0.09925	226.2
							Af_9	Af_{10}	Af_{11}	Af_{12}	Af_{13}	Af_{14}	Af_{15}		
							0.001837	0.05019	0.2328	0.8459	0.3286	0.6283	0.05152		
8	80	25	20	0.8	0.05	1	Af_1	Af_2	Af_3	Af_4	Af_5	Af_6	Af_7	Af_8	*STL*(dB)
							0.7865	0.1477	0.191	0.2494	0.2587	0.2941	0.00505	0.08529	239.3
							Af_9	Af_{10}	Af_{11}	Af_{12}	Af_{13}	Af_{14}	Af_{15}		
							0.004183	0.03835	0.2041	0.3451	0.4518	0.2828	0.06884		
9	80	25	25	0.8	0.05	1	Af_1	Af_2	Af_3	Af_4	Af_5	Af_6	Af_7	Af_8	*STL*(dB)
							0.7633	0.1491	0.1999	0.2744	0.322	0.2017	0.002304	0.09473	229.4
							Af_9	Af_{10}	Af_{11}	Af_{12}	Af_{13}	Af_{14}	Af_{15}		
							0.004152	0.04984	0.3676	0.3793	0.226	0.2643	0.06922		
10	80	25	30	0.8	0.05	1	Af_1	Af_2	Af_3	Af_4	Af_5	Af_6	Af_7	Af_8	*STL*(dB)
							0.7824	0.1476	0.1703	0.2275	0.2258	0.2017	0.001971	0.09254	233.2
							Af_9	Af_{10}	Af_{11}	Af_{12}	Af_{13}	Af_{14}	Af_{15}		
							0.005984	0.04382	0.2342	0.575	0.2417	0.4258	0.05325		
11	100	25	20	0.8	0.05	1	Af_1	Af_2	Af_3	Af_4	Af_5	Af_6	Af_7	Af_8	*STL*(dB)
							0.7484	0.1739	0.1931	0.2713	0.2733	0.2751	0.003233	0.09843	244.2
							Af_9	Af_{10}	Af_{11}	Af_{12}	Af_{13}	Af_{14}	Af_{15}		
							0.003454	0.05956	0.2178	0.2924	0.4087	0.2075	0.06152		
12	120	25	20	0.8	0.05	1	Af_1	Af_2	Af_3	Af_4	Af_5	Af_6	Af_7	Af_8	*STL*(dB)
							0.7642	0.1747	0.1856	0.2118	0.2023	0.2196	0.004501	0.06804	245.4
							Af_9	Af_{10}	Af_{11}	Af_{12}	Af_{13}	Af_{14}	Af_{15}		
							0.00409	0.03479	0.2773	0.2007	0.2801	0.2164	0.05652		
13	120	50	20	0.8	0.05	1	Af_1	Af_2	Af_3	Af_4	Af_5	Af_6	Af_7	Af_8	*STL*(dB)
							0.6519	0.1481	0.195	0.125	0.2117	0.2589	0.002494	0.09802	251.4
							Af_9	Af_{10}	Af_{11}	Af_{12}	Af_{13}	Af_{14}	Af_{15}		
							0.003628	0.05826	0.278	0.2281	0.3129	0.2513	0.07942		
14	**120**	**100**	**20**	**0.8**	**0.05**	**1**	Af_1	Af_2	Af_3	Af_4	Af_5	Af_6	Af_7	Af_8	*STL*(dB)
							0.7455	**0.1723**	**0.1626**	**0.2384**	**0.2123**	**0.2205**	**0.004957**	**0.09767**	**293.8**
							Af_9	Af_{10}	Af_{11}	Af_{12}	Af_{13}	Af_{14}	Af_{15}		
							0.006661	**0.0313**	**0.3232**	**0.4963**	**0.3054**	**0.2157**	**0.06763**		

Table 4. Optimal design parameters and *STL*s for three kinds of mufflers (muffler (A), muffler (B), and muffler (C)) at targeted tone (300 Hz).

Muffler type	Design parameters										Result
Muffler (A)	Af_1	Af_2	Af_3	Af_4	Af_5	Af_6	Af_7	Af_8	Af_9		STL(dB)
	0.6686	0.1317	0.1416	0.1782	0.5411	0.2903	0.00590	0.08659	0.00352		525.8
	Af_{10}	Af_{11}	Af_{12}	Af_{13}	Af_{14}	Af_{15}	Af_{16}	Af_{17}	Af_{18}		
	0.05285	0.00271	0.0968	0.00667	0.03123	0.5428	0.4381	0.6133	0.09178		
Muffler (B)	Af_1	Af_2	Af_3	Af_4	Af_5	Af_6	Af_7	Af_8			STL(dB)
	0.7455	0.1723	0.1626	0.2384	0.2123	0.2205	0.00495	0.09767			293.8
	Af_9	Af_{10}	Af_{11}	Af_{12}	Af_{13}	Af_{14}	Af_{15}				
	0.00666	0.0313	0.3232	0.4963	0.3054	0.2157	0.06763				
Muffler (C)	Af_1	Af_2	Af_3	Af_4	Af_5	Af_6	Af_7	Af_8	Af_9	Af_{10}	STL(dB)
	0.7633	0.1701	0.1479	0.2713	0.2214	0.3841	0.4251	0.4142	0.4073	0.08297	192.1

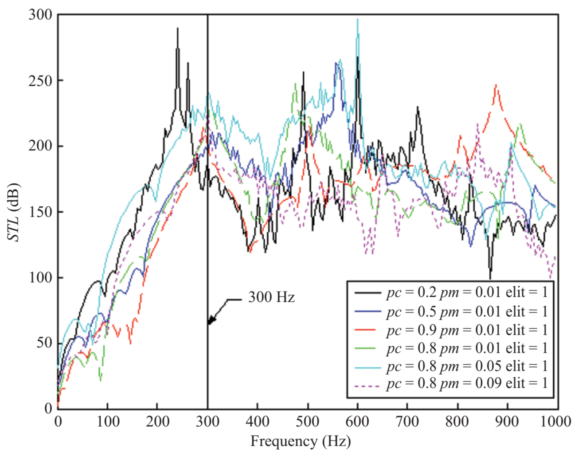

Fig. 9. *STL*s with respect to frequency at various *pc* and *pm* (*gen*: 25; *bit*: 10; *pop*: 80; *gen*: 25; target tone of 300 Hz) (muffler (B); f_c = 996 Hz).

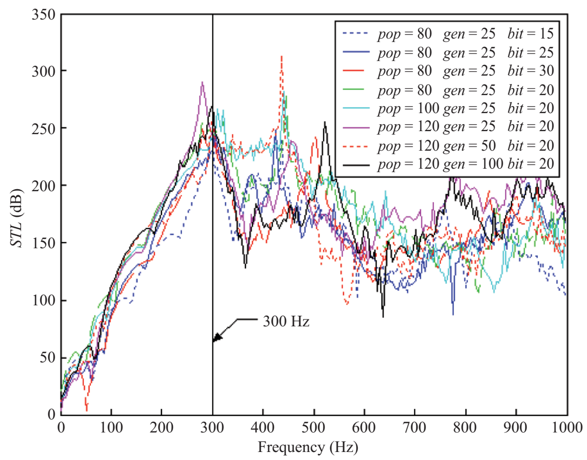

Fig. 10. *STL*s with respect to frequency at various *pop*, *gen*, and *bit* (*pc*: 0.8; *pm*: 0.05; target tone of 300 Hz) (muffler (B); f_c = 996 Hz).

VI. RESULTS AND DISCUSSION

1. Results

To achieve an acceptable optimization, five kinds of optimal *GA* parameters, including population size (*pop*), chromosome length (*bit*), maximum generation (*gen*), crossover ratio (*pc*), and mutation ratio (*pm*), are obtained by varying their values during optimization. The results of shaped mufflers at various targeted tones are described below.

1) Pure Tone Noise Optimization

A. Pure Tone Noise Optimization at 300 Hz (muffler (A), muffler (B), and muffler (C))

For a five-chamber side inlet/outlet muffler equipped with two perforated and two non-perforated intruding tubes (muffler (B)), various sets of *GA* parameters are tested by using the formulas of Eq. (31) during the optimal process. The resultant simulated result optimized with respect to the pure tone of 300 Hz is shown in Table 3. As indicated in Table 3, the optimal design data can be obtained when the *GA* parameters at *pop*, *bit*, *gen*, *pc*, and *pm* = 120, 20, 100, 0.8, 0.05 are applied. The optimal *STL*s with respect to various *GA* parameters (*pop*, *bit*, *gen*, *pc*, and *pm*) are plotted in Figs. 9 and 10.

By using the above *GA* parameters, the optimal muffler's design data for two kinds of side inlet/outlet mufflers (muffler (A) and muffler (C)) used to maximize the mufflers' sound transmission loss at 300 Hz is performed. The optimal design parameters and *STL*s are summarized in Table 4. Three optimal *STL*s with respect to various mufflers (muffler (A), muffler (B), and muffler (C)) are plotted in Fig. 11.

B. Pure Tone Noise Optimization at 600 Hz and 900 Hz (muffler (B) and muffler (C))

Using the formulas of Eq. (33) and the above *GA* parameter set in muffler (B), the optimized design data at the targeted tones (600 Hz and 900 Hz) are performed. The resultant data with respect to three tones is summarized in Table 5. Using the optimal design in a theoretical calculation, three optimal *STL* curves with respect to the targeted frequencies are plotted and depicted in Fig. 12. Moreover, using the formulas of

Table 5. Optimal design parameters and *STL*s at three tones (300 Hz, 600 Hz, and 900 Hz) (muffler (B)).

Targeted tone (Hz)	Design parameters								Result
300	Af_1	Af_2	Af_3	Af_4	Af_5	Af_6	Af_7	Af_8	STL(dB)
	0.7455	0.1723	0.1626	0.2384	0.2123	0.2205	0.004957	0.09767	293.8
	Af_9	Af_{10}	Af_{11}	Af_{12}	Af_{13}	Af_{14}	Af_{15}		
	0.006661	0.0313	0.3232	0.4963	0.3054	0.2157	0.06763		
600	Af_1	Af_2	Af_3	Af_4	Af_5	Af_6	Af_7	Af_8	STL(dB)
	0.5865	0.1108	0.1417	0.5254	0.5331	0.2947	0.003469	0.09391	385.6
	Af_9	Af_{10}	Af_{11}	Af_{12}	Af_{13}	Af_{14}	Af_{15}		
	0.003854	0.08734	0.3197	0.4593	0.2417	0.2068	0.07408		
900	Af_1	Af_2	Af_3	Af_4	Af_5	Af_6	Af_7	Af_8	STL(dB)
	0.7871	0.1499	0.09443	0.2806	0.7543	0.2276	0.001863	0.07455	402.8
	Af_9	Af_{10}	Af_{11}	Af_{12}	Af_{13}	Af_{14}	Af_{15}		
	0.00524	0.0794	0.3006	0.3704	0.2062	0.2684	0.09687		

Table 6. Optimal design parameters and *STL*s at three tones (300 Hz, 600 Hz, and 900 Hz) (muffler (C)).

Targeted tone (Hz)	Design parameters					Result
300	Af_1	Af_2	Af_3	Af_4	Af_5	STL(dB)
	0.7633	0.1701	0.1479	0.2713	0.2214	192.1
	Af_6	Af_7	Af_8	Af_9	Af_{10}	
	0.3841	0.4251	0.4142	0.4073	0.08297	
600	Af_1	Af_2	Af_3	Af_4	Af_5	STL(dB)
	0.6308	0.1162	0.1422	0.5559	0.2835	437.8
	Af_6	Af_7	Af_8	Af_9	Af_{10}	
	0.6468	0.3553	0.4648	0.4929	0.08524	
900	Af_1	Af_2	Af_3	Af_4	Af_5	STL(dB)
	0.5387	0.1540	0.09478	0.6537	0.2060	312.9
	Af_6	Af_7	Af_8	Af_9	Af_{10}	
	0.3225	0.2479	0.4559	0.3156	0.06114	

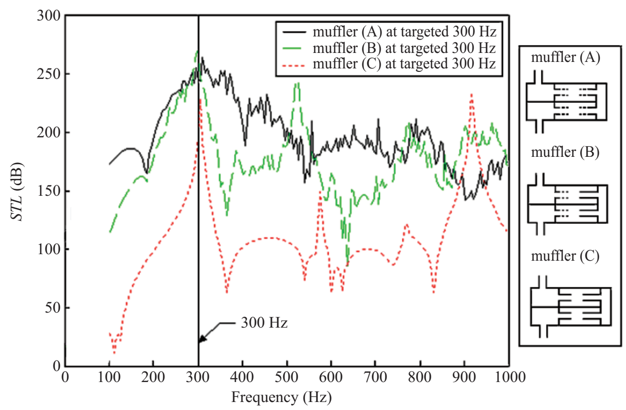

Fig. 11. Comparison of *STL*s with respect to three kinds of side inlet/outlet mufflers at the target tone of 300 Hz (A: four perforated intruding tubes (f_c = 996 Hz); B: two perforated and two non-perforated intruding tubes (f_c = 996 Hz); C: four non-perforated intruding tubes (f_c = 996 Hz)).

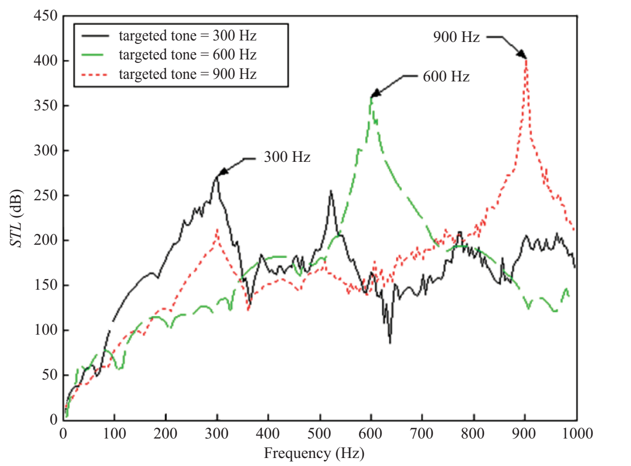

Fig. 12. Comparison of *STL*s with respect to three targeted tones (300 Hz, 600 Hz, and 900 Hz) (muffler (B); f_c = 996 Hz).

Eq. (35) and the same *GA* parameters in optimizing muffler (C) at the targeted tones (600 Hz and 900 Hz), the resultant data with respect to three tones is summarized in Table 6. Also, using the optimal design in a theoretical calculation, three optimal *STL* curves with respect to targeted frequencies are plotted and depicted in Fig. 13.

Table 7. Optimal design parameters and SWL_T for three kinds of mufflers (muffler (A), muffler (B), and muffler (C)) (broadband noise).

Muffler type	Design parameters									Result
Muffler (A)	Af_1	Af_2	Af_3	Af_4	Af_5	Af_6	Af_7	Af_8	Af_9	SWL_T(dB)
	0.6343	0.1233	0.1010	0.3956	0.7475	0.2242	0.00415	0.07872	0.00327	35.8
	Af_{10}	Af_{11}	Af_{12}	Af_{13}	Af_{14}	Af_{15}	Af_{16}	Af_{17}	Af_{18}	
	0.07065	0.00196	0.0767	0.00425	0.07065	0.5223	0.7953	0.5196	0.08134	
Muffler (B)	Af_1	Af_2	Af_3	Af_4	Af_5	Af_6	Af_7	Af_8		SWL_T(dB)
	0.6909	0.1441	0.1471	0.2693	0.5016	0.2636	0.00470	0.07631		59.3
	Af_9	Af_{10}	Af_{11}	Af_{12}	Af_{13}	Af_{14}	Af_{15}			
	0.00407	0.05677	0.5910	0.6124	0.5504	0.4411	0.07267			
Muffler (C)	Af_1	Af_2	Af_3	Af_4	Af_5	Af_6	Af_7	Af_8	Af_9	Af_{10}	SWL_T(dB)
	0.6932	0.1285	0.1488	0.2235	0.2851	0.2928	0.7803	0.5866	0.2514	0.07759	66.2

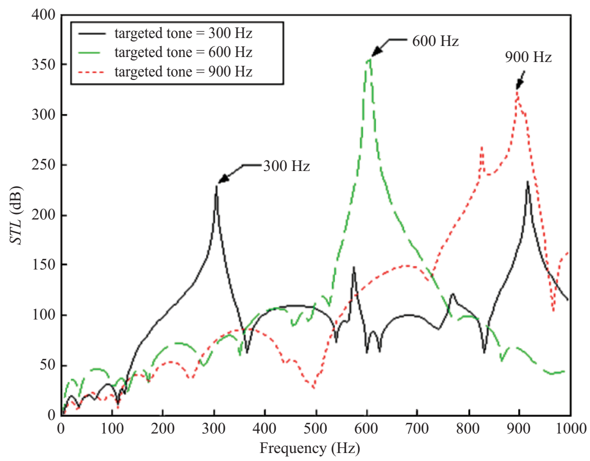

Fig. 13. Comparison of *STL*s with respect to three targeted tones (300 Hz, 600 Hz, and 900 Hz) (muffler (C); f_c = 996 Hz).

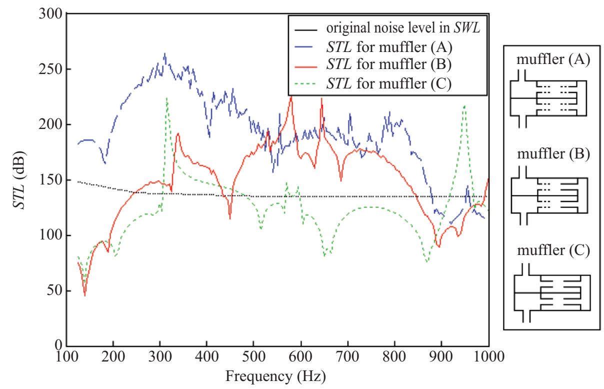

Fig. 14. Comparison of *STL*s with respect to various mufflers (f_c for mufflers A, B, and C are 996 Hz) (broadband noise).

2) Broadband Noise Optimization

By using the formulas of Eqs. (32) (34) (36) and the *GA* parameters of *pop* = 120, *bit* = 20, *gen* = 100, *pc* = 0.8, *pm* = 0.05, three kinds of optimal design parameters for minimizing the sound power level at the muffler's outlet within a limited space are shown in Table 7 and plotted in Fig. 14. The resultant sound power levels with respect to three kinds of mufflers have been dramatically reduced from 148.8 dB to 35.8 dB, 59.8 dB, and 66.2 dB.

2. Discussion

To achieve sufficient optimization, the selection of the appropriate *GA* parameter set is essential. As indicated in Table 3 and Figs. 9~10, the best *GA* sets with respect to muffler (B) — a five-chamber side inlet/outlet muffler equipped with two perforated and two non-perforated intruding tubes — at the targeted pure tone noise of 300 Hz are shown. Also, using the *GA* parameter set in various mufflers (muffler (A) and muffler (C)) and applying the optimal design in a theoretical calculation, three optimal *STL* curves with respect to various mufflers are obtained and shown in Fig. 11. Fig. 11 reveals that mufflers equipped with perforated intruding tubes (muffler (A) and muffler (B)) are superior to those equipped with non-perforated intruding tubes (muffler (C)). Moreover, mufflers with multi-perforated tubes will increase the acoustic performance at the targeted frequency.

As can be observed in Tables 5~6 and Figs. 12~13, the *STL*s are maximized at the desired frequencies (300 Hz, 600 Hz, and 900 Hz). Therefore, using the *GA* optimization to find a better design solution is seen to be reliable. In addition, it has been found that the acoustical performance for a side inlet/outlet muffler equipped with multi-perforated tubes is much better than mufflers equipped with non-perforated tubes. Moreover, the tuned tone band for a side inlet/outlet muffler equipped with multi-perforated tubes is much wider than mufflers equipped with non-perforated tubes. Also, the acoustical performance at a higher targeted tone will increase.

Additionally, in dealing with the broadband noise (125 Hz~1000 Hz) using the above mufflers, the *GA*'s solution shown in Table 7 and Fig. 14 can also provide the appropriate and sufficient sound reduction within a constrained space. As indicated in Table 7, the overall noise reductions with respect to three kinds of mufflers (muffler (A), muffler (B), and muffler (C)) can reach 113 dB, 89 dB, and 82.6 dB. As shown in Fig. 14, the whole acoustical performance of muffler (A) is superior to that of other mufflers. It has been seen that the acoustical performance for a side inlet/outlet muffler equipped with multi-perforated tubes is much better than that of mufflers equipped with non-perforated tubes.

VII. CONCLUSION

It has been shown that five-chamber side inlet/outlet mufflers hybridized with perforated/non-perforated intruding-tubes in conjunction with a *GA* optimizer can be easily and efficiently optimized within a constrained space by using a generalized decoupling technique, a plane wave theory, as well as a four-pole transfer matrix. Five kinds of *GA* parameters (*pop*, *bit*, *gen*, *pc*, and *pm*) play essential roles in the solution's accuracy during *GA* optimization. As indicated in Figs. 11~13, the tuning ability established by adjusting the design parameters of five-chamber side inlet/outlet mufflers hybridized with perforated/non-perforated intruding-tubes is reliable. Moreover, as indicated in Table 4 and Fig. 11, the acoustical performances of the mufflers having perforated intruding tubes (muffler (A) and muffler (B)) are higher than those having non-perforated intruding tubes (muffler (C)). It has also been found that the acoustic performance of the muffler will increase at the targeted frequency when the perforated tubes are increased.

As can be seen in Figs. 12~13, the tuned tone band for a side inlet/outlet muffler having more perforated tubes is much wider and higher than mufflers having non-perforated tubes. Simulated results indicate that the mufflers have better acoustical performance at a higher targeted tone compared to the lower targeted tones.

In addition, using the acoustical treatment in the broadband noise, the *GA*'s solution shown in Fig. 14 can also provide adequate noise reduction by adjusting the design data in conjunction with the *GA* optimizer. Table 7 reveals that the overall noise reductions with respect to three kinds of mufflers are 113 dB, 89 dB, and 82.6 dB. This means that the acoustical performance for a side inlet/outlet muffler having multi-perforated tubes is indeed superior to those mufflers having non-perforated tubes.

Consequently, the approach used for the optimal design of the side inlet/outlet mufflers equipped with multiple open-ended perforated/non-perforated intruding tubes proposed in this study is quite efficient in dealing with industrial venting noise within a constrained space.

NOMENCLATURE

This paper is constructed on the basis of the following notations:

bit	bit length
C_o	sound speed (m s^{-1})
dh_i	the diameter of a perforated hole on the i-th inner tube (m)
D_i	diameter of the i-th tubes (m)
D_o	diameter of the outer tube (m)
elt	elitism (1 for yes, 0 for no)
f	cyclic frequency (Hz)
f_c	cut-off frequency of plane wave (Hz)
gen	maximum iteration
j	imaginary unit
k	wave number ($=\frac{\omega}{c_o}$)
L_i	length of the ith segment of a muffler (m)
L_o	total length of the muffler (m)
M	mean flow Mach number
OBJ_i	objective function (dB)
pc	crossover ratio
p_i	acoustic pressure at the i-th node (Pa)
pm	mutation ratio
pop	number of population
Q	volume flow rate of venting gas (m^3 s^{-1})
S_i	section area at the i-th node (m^2)
STL	sound transmission loss (dB)
$SWLO_i$	the original *SWL* with respect to i-th octave band frequency at the inlet of the muffler (dB)
$[T_m(f)]$	components of four-pole transfer matrices for the m-th acoustical mechanism
$T^*_{ij}, T^{**}_{ij}, T^{***}_{jj}$	components of a four-pole transfer system matrices
u_i	acoustic particle velocity at the i-th node (m s^{-1})
ρ_o	air density (kg m^{-3})
ρ_i	acoustical density at the i-th node
sgm_i	the porosity of the i-th inner perforated tube.

ACKNOWLEDGMENTS

The authors acknowledge the financial support of the National Science Council (NSC97-2221-E-235-001, Taiwan, ROC).

REFERENCES

1. Chang, Y. C., Yeh, L. J., and Chiu, M. C., "Numerical studies on constrained venting system with side inlet/outlet mufflers by GA optimization," *Acta Acustica united with Acustica*, Vol. 90, No. 1-1, pp. 1-11 (2004).
2. Chang, Y. C., Yeh, L. J., and Chiu, M. C., "GA optimization on single-chamber muffler hybridized with extended tube under space constraints," *Archives of Acoustics*, Vol. 29, No. 4, pp. 577-596 (2004).
3. Chiu, M. C., "Shape optimization of double-chamber side mufflers with extended tube by using four-pole matrix and simulated annealing method," *Journal of Mechanics*, Vol. 4, pp. 31-43 (2008).
4. Chiu, M. C., Yeh, L. J., Chang, Y. C., and Lan, T. S., "Shape optimization of single-chamber mufflers with side inlet/outlet by using boundary element method, mathematic gradient method and genetic algorithm," *Tamkang Journal of Science and Engineering*, Vol. 12, No. 1, pp. 85-98 (2009).

5. Davis, D. D., Stokes, J. M., and Moorse, L., “Theoretical and experimental investigation of mufflers with components on engine muffler design,” NACA Report 1192 (1954).
6. Holland, J., *Adaptation in Natural and Artificial System*, University of Michigan Press, Ann Arbor (1975).
7. Jayaraman, K. and Yam, K., “Decoupling approach to modeling perforated tube muffler component,” *Journal of Acoustical Society of America*, Vol. 69, No. 2, pp. 390-396 (1981).
8. Jong, D., *An Analysis of the Behavior of a Class of Genetic Adaptive Systems*, Doctoral Thesis, Department of Computer and Communication Sciences, University of Michigan, Ann Arbor (1975).
9. Magrab, E. B., *Environmental Noise Control*, John Wiley and Sons, New York (1975).
10. Munjal, M. L., *Acoustics of Ducts and Mufflers with Application to Exhaust and Ventilation System Design*, John Wiley & Sons, New York (1987).
11. Munjal, M. L., “Plane wave analysis of side inlet/outlet chamber mufflers with mean flow,” *Applied Acoustics*, Vol. 52, pp. 165-175 (1997).
12. Munjal, M. L., Rao, K. N., and Sahasrabudhe, A. D., “Aeroacoustic analysis of perforated muffler components,” *Journal of Sound and Vibration*, Vol. 114, No. 2, pp. 173-188 (1987).
13. Peat, K. S., “A numerical decoupling analysis of perforated pipe silencer elements,” *Journal of Sound and Vibration*, Vol. 123, No. 2, pp. 199-212 (1988).
14. Rao, K. N. and Munjal, M. L., “Experimental evaluation of impedance of perforates with grazing flow,” *Journal of Sound and Vibration*, Vol. 123, pp. 283-295 (1986).
15. Sathyanarayana, Y. and Munjal, M. L., “A hybrid approach for aeroacoustic analysis of the engine exhaust system,” *Applied Acoustics*, Vol. 60, pp. 425-450 (2000).
16. Sullivan, J. W., “A method of modeling perforated tube muffler components I: Theory,” *Journal of the Acoustical Society of America*, Vol. 66, pp. 772-778 (1979).
17. Sullivan, J. W., “A method of modeling perforated tube muffler components II: Applications,” *Journal of the Acoustical Society of America*, Vol. 66, pp. 779-788 (1979).
18. Sullivan, J. W. and Crocker, M. J., “Analysis of concentric tube resonators having unpartitioned cavities,” *Journal of the Acoustical Society of America*, Vol. 64, pp. 207-215 (1978).
19. Thawani, P. T. and Jayaraman, K., “Modeling and applications of straight-through resonators,” *Journal of Acoustical Society of America*, Vol. 73, No. 4, pp. 1387-1389 (1983).
20. Wang, C. N., *The Application of Boundary Element Method in the Noise Reduction Analysis for the Automotive Mufflers*, Doctoral Thesis, Taiwan University (1992).
21. Wang, C. N., “A numerical scheme for the analysis of perforated intruding tube muffler components,” *Applied Acoustics*, Vol. 44, pp. 275-286 (1995).
22. Yeh, L. J., Chang, Y. C., Chiu, M. C., and Lai, G. J., “Computer-aided optimal design of a single-chamber muffler with side inlet/outlet under space constraints,” *Journal of Marine Science and Technology*, Vol. 11, No. 4, pp. 1-8 (2003).